JOURNAL OF Materials CHEMISTRY

Synthesis, characterisation, and fluorescence spectroscopic mobility studies of fluorene labeled inorganic–organic hybrid polymers[1]

Hans-Joachim Egelhaaf,[a] Elisabeth Holder,[b] Petr Herman,[c] Hermann A. Mayer,[b] Dieter Oelkrug[a] and Ekkehard Lindner*[b]

[a]*Institut für Physikalische und Theoretische Chemie der Universität Tübingen, Auf der Morgenstelle 8, 72076 Tübingen, Germany*
[b]*Institut für Anorganische Chemie der Universität Tübingen, Auf der Morgenstelle 18, D-72076 Tübingen, Germany. E-mail: ekkehard.lindner@uni-tuebingen.de*
[c]*Center for Fluorescence Spectroscopy, University of Maryland School of Medicine, 725 West Lombard St., Baltimore, Md., U.S.A.*

Received 6th March 2001, Accepted 26th June 2001
First published as an Advance Article on the web 13th August 2001

In the attempt to find catalyst supports with improved accessibilities for tethered transition metal complexes, a series of inorganic–organic hybrid polymers was synthesised by sol–gel processing of three different silyl-functionalised alkyl derivatives. The resulting materials were characterised by solid-state NMR spectroscopy, BET measurements and elemental analysis. Molecular mobilities in the solvent-swollen polymers were determined by fluorescence spectroscopy. As fluorescent probe, fluorene was covalently attached to the polymer matrix by a T-silyl-functionalised alkyl spacer. The rotational mobilities of the probe were determined by steady-state and time-resolved fluorescence depolarisation experiments. Translational mobilities of molecular species dissolved in the liquid phase were investigated by the kinetics of luminescence quenching after pulsed laser excitation. Both rotational and translational mobilities in hybrid materials are significantly higher than in conventional Q-type polysiloxanes. However, the mobilities are still about one to two orders of magnitude lower than in homogeneous solutions, and thus contribute to the reduced accessibilities of matrix bound transition metal catalysts. The highest mobilities were observed in dichloromethane and organic ethers, which have the strongest swelling capabilities for the hybrid polymers. Compared to D-silyl polymers, mobilities in T-silyl based materials are significantly higher.

1. Introduction

Sol–gel processed polysiloxanes are widely investigated as potential supports for reporter molecules in chemical sensors.[2,3] However, only little use has been made of sol–gel processed polymeric materials as supports for catalytically active transition metal complexes.[4,5] Upon swelling of the polymer in appropriate solvents, an interphase is formed, where solid and liquid phases interpenetrate on the molecular level without forming a homogeneous solution. Ideally, these materials combine the convenient handling of solids with the molecular dispersity of the active sites encountered in homogeneous solutions. Real samples suffer from several problems, among which chemical stability and accessibility of the active centers are the most serious ones. Decomposition of the matrix is reduced by increasing the cross-linking of the polymer, *i.e.*, by using tri- (T) or quater- (Q) functionalised silanes. Leaching of the active centers is impeded by covalently binding them to the matrix *via* long-chain T-silyl functionalised spacers and by the employment of polyfunctionalised ligands. However, by increasing the cross-linking of the material, the swelling of the polymer in liquids is reduced, which leads to diffusion problems and greatly diminished accessibility of the active centers for reactant molecules dissolved in the liquid phase. A possible approach to resolve this dilemma is to employ hybrid polymers instead of pure polysiloxanes. In these hybrid polymers, which are employed by our group as solid supports for tethered transition metals complex catalysts, the functionalised silanes **3**[=**2**(**T**^{0})] (Schemes 1 and 2) are subjected to the sol–gel process together with the co-condensation agents **4**[=**MeT**^{0}], **5**[=**T**^{0}**C**$_6$**T**^{0}], and **6**[=**D**^{0}**C**$_6$**D**^{0}] (Scheme 2). The siloxane groups provide the desired degree of cross-linking, while the organic substituents of the co-condensation agents are supposed to enhance the swelling ability of the hybrid polymers.

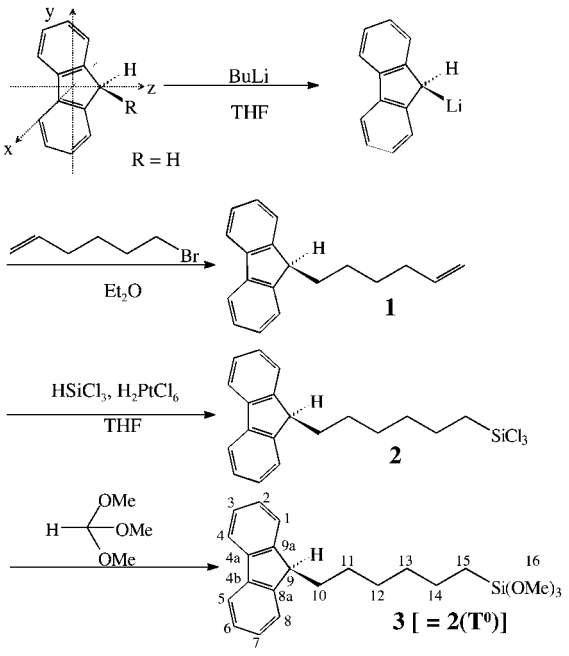

Scheme 1

DOI: 10.1039/b102088i

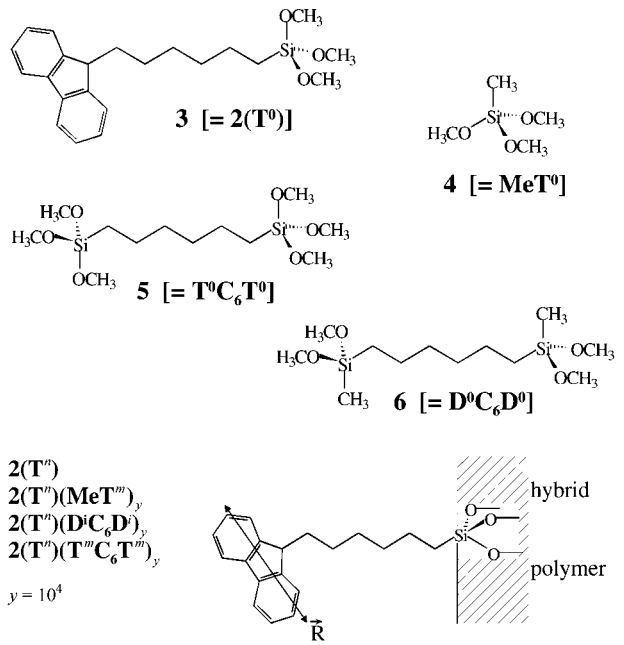

$\vec{R}$ = transition dipole moment

T = T type silicon atom (three oxygen neighbors)

D = D type silicon atom (two oxygen neighbors)

n, *m*, *i* = number of Si-O-Si bonds (*n* = 0-3; *m* = 0-3; *i* = 0-2)

y = molar ratio of co-condensate and **2(T^n)**

Scheme 2

Optimisation of stationary phases requires quantification of the accessibility of the active centers bound to the matrix and of the diffusional mobility of reactants dissolved in the liquid phase. A variety of spectroscopic techniques, including NMR and UV/Vis spectroscopy, has been applied for this purpose. NMR spectroscopy provides mainly information on the polymeric matrix and highly concentrated active centers.[6,7] For the investigation of species present in the interphase at low concentrations, the highly sensitive UV/Vis fluorescence spectroscopy is more appropriate. Ample use has been made of fluorescent probes to characterise the microenvironment in sol–gel processed materials.[8–21] The vast majority of these publications deals with probe molecules sequestered within the matrix, while only few studies employ covalently attached probes.[22–34]

In this work, fluorene is attached covalently to organic–inorganic hybrid polymers as a fluorescent model compound for matrix bound active centers. We are thus able to investigate quantitatively the mobility in the interphase by fluorescence spectroscopic methods. The rotational mobility of the fluorene labels is probed by steady-state and time-resolved fluorescence depolarisation. The translational mobility of low molecular weight species dissolved in the mobile component is probed by the kinetics of exciplex formation between fluorene and triethylamine. These experiments provide a detailed picture of the factors affecting the accessibility of matrix bound active centers by molecules dissolved in the mobile phase. The insight thus gained will be useful in the synthesis of new hybrid catalysts with improved turn over rates.

2. Experimental

2.1. Syntheses

Elemental analyses were carried out on a Vario EL analyzer (Fa. Elementar Analytische Systeme, Hanau). Solution and suspension nuclear magnetic resonance spectra (NMR) were recorded on a Bruker DRX 250 spectrometer at 298 K. Frequencies and standards were as follows: ^{1}H NMR, 250.13 MHz; ^{13}C{^{1}H} NMR, 62.90 MHz. All NMR spectra were calibrated relative to partially deuterated solvent peaks which are reported relative to tetramethylsilane (TMS). EI mass spectra were acquired on a Finnigan TSQ 70 instrument and are reported as mass/charge (*m*/*z*). IR data were obtained on a Bruker IFS 48 FT-IR spectrometer. BET surfaces and pore volumes were obtained with a Coulter SA3100 (Beckman Coulter GmbH), measuring the adsorption and desorption isotherms after drying the samples for 12 h at $T = 50\,^{\circ}$C under vacuum. Measurements of fluorescence anisotropy before and after the BET experiments yield the same results and thus exclude major changes of the pore structure by the drying procedure.

CP/MAS solid state NMR spectra were recorded on Bruker DSX 200 (4.7 T) (^{29}Si) and ASX 300 (7.05 T) (^{13}C) multinuclear spectrometers equipped with wide-bore magnets. Magic angle spinning was applied at 3.5 kHz (^{29}Si) and 10 kHz (^{13}C), respectively. All samples were packed under exclusion of molecular oxygen. Frequencies and standards: ^{29}Si, 39.75 MHz (Q_8M_8); ^{13}C, 75.47 MHz [TMS, carbonyl resonance of glycine (δ 170.09) as the second standard]. No relative intensities are given for ^{29}Si NMR spectra, due to the different efficiencies of magnetisation transfer to inequivalent ^{29}Si nuclei.

All manipulations were performed under an atmosphere of dry argon by employing standard Schlenk techniques. The solvents were dried according to common methods, distilled, and stored under argon. 9-(Hex-5′-enyl)-9*H*-fluorene (**1**)[35] and the co-condensation agents **T^{0}C$_6$T^0**,[36] and **D^{0}C$_6$D^0**[37] were synthesised according to literature methods. **MeT^0** was purchased from Fluka.

2.1.1. 6-(9*H*-Fluorenyl)hexyltrimethoxysilane. 9-(Hex-5′-enyl)-9*H*-fluorene (**1**) (8.00 g, 32.0 mmol) was treated with trichlorosilane (4.0 mL, 40.00 mmol) and a suspension of hexachloroplatinic acid (15.0 mg, 2.9×10^{-2} mmol) in 25 mL of THF. The mixture was stirred for 48 h at 20 °C and a dark brown solution was formed. This solution was added dropwise to trimethyl orthoformate (11.5 mL, 105.00 mmol) and the mixture was stirred overnight at room temperature. The volatile components of the solution were removed *in vacuo* and the residual oil was purified on a silica gel column (length 15 cm, diameter 4 cm, solvents: *n*-hexane, toluene, and THF): yield 8.52 g (71.8%); ^{13}C{^{1}H} NMR ($CDCl_3$, for labeling and assignment see Scheme 1 and ref. 35) 148.5 (s, C9a, C8a), 142.0 (s, C5a, C4a), 127.8 (s, C3, C6), 127.7 (s, C2, C7), 125.2 (2, C1, C8), 120.7 (s, C4, C5), 51.4 (s, C16), 48.4 (s, C9), 34.0 (s, C10), 33.7 (s, C13), 30.4 (s, C12), 26.4 (s, C11), 23.4 (s, C14), 9.9 (s, C15); ^{1}H NMR ($CDCl_3$, for labeling and assignment see Scheme 1 and ref. 35) 7.74 (d, $^2J_{CH} = 6.6$ Hz, 2H, C1H, C8H), 7.50 (d, $^2J_{CH} = 6.9$ Hz, 2H, C4H, C5H), 7.34–7.10 (m, 4H, C2H, C3H, C6H, C7H), 3.95–3.92 (m, 1H, C9H), 3.41 (s, 9H, C16H), 1.99–1.95 (m, 2H, C10H), 1.60 (m, 2H, C11H), 1.32–1.17 (m, 6H, C12H, C13H, C14H), 0.60–0.54 (m, 2H, C15H); EI-MS *m*/*z* 370.2 [M$^+$]. Anal. Calcd for $C_{22}H_{30}O_3Si$: C, 71.31; H, 8.16. Found: C, 71.29; H, 6.72%.

2.1.2. Sol–gel processing of 2(T^0) with different co-condensation agents—general procedure. The silane **2(T^0)** was polycondensed by itself and with the co-condensation agents **MeT^0**, **T^{0}C$_6$T^0**, and **D^{0}C$_6$D^0** (Scheme 2) in a molar ratio of $1 : 10^4$. An appropriate mixture of the respective T^0 and D^0 functionalised monomeric silanes with water, methanol and a catalyst was stirred for 12 h at 30 °C until the gels precipitated. Subsequently the solvent was removed under reduced pressure and the resulting gels were dried for 4 h *in vacuo*. Solvent processing was performed by vigorously stirring the large gel particles in

10 mL of *n*-hexane overnight. The wet gels were triturated and washed twice with 20 mL of *n*-hexane, methanol, and dichloromethane and dried *in vacuo* for 4 h. Before starting the fluorescence measurements on these samples, they were allowed to sit for two weeks at room temperature.

2.1.3. Preparation of the polysiloxane 2(T^n). A mixture of **2(T^0)** (560 mg, 1.51 mmol), methanol (2.5 mL), water (250 μL), and ammonia (250 μL of a 0.1 m solution) as catalyst was sol–gel processed; yield 400 mg (71.4%); $^{13}C\{^1H\}$ NMR (suspension in $CDCl_3$, for labeling and assignment see Scheme 1 and ref. 35) 146.5 (s, C9a, C8a), 140.0 (s, C5a, C4a), 125.8 (s, C3, C6), 125.7 (s, C2, C7), 123.3 (s, C1, C8), 118.7 (s, C4, C5), 46.4 (s, C16), 43.8 (s, C9), 32.2 (s, C10), 32.1 (s, C13), 28.6 (s, C12), 23.9 (s, C11), 22.1 (s, C14), 10.6 (s, C15); ^1H NMR (suspension in $CDCl_3$, for labeling and assignment see Scheme 1 and ref. 35) 7.56 (m, 2H, C1H, C8H), 7.30 (m, 2H, C4H, C5H), 7.14 (m, 4H, C2H, C3H, C6H, C7H), 3.92 (m, 1H C9H), 3.32 (m, H, C16H), 1.80 (m, 2H, C10H), 1.53 (m, 2H, C11H), 1.05 (m, 6H, C12H, C13H, C14H), 0.58 (m, 2H, C15H); IR (KBr, cm^{-1}) 3445 m [ν(OH)], 3064 w, 3039 w [$\nu(C–H)_{aromat.}$], 2931 sst [$\nu(CH_2)$], 2858 st [$\nu(OCH_3)$], 1739 w, 1611 w [$\nu(C{=}C)_{aromat.}$], 1477 m, 1449 s [$\delta(CH_2)$], 1262 m, 1193 m [$\nu(SiCH_2)$], 1111 sst [$\nu(Si_2O)$], 917 w [$\nu(SiOCH_3)$].

2.1.4. Preparation of the polysiloxane 2(T^n)(MeT^m)$_y$. A mixture of **2(T^0)** (0.4 mg, 1.08×10^{-3} mmol), **MeT^0** (1.36 g, 10.02 mmol), 5 mL of methanol, 500 μL of water, and 500 μL (0.1 mol) of ammonia was sol–gel processed: yield 1.20 g (88.2%); ^{13}C CP/MAS NMR 49.5 ($SiOCH_3$), −0.4 ($SiCH_3$); ^{29}Si CP/MAS NMR (silicon substructure) −56.2 (T^2), −65.6 (T^3). Anal. Calcd for $C_{19}H_{21}O_{1.5}Si(CH_3O_{1.5}Si)_{10000}$: C, 17.93; H, 4.51. Found: C, 13.84; H, 4.60%. BET surface $A_{BET}=0.56\ m^2\ g^{-1}$.

2.1.5. Preparation of the polysiloxane 2(T^n) (D^{i}C$_6$D^i)$_y$. A mixture of **2(T^0)** (0.75 mg, 2.02×10^{-3} mmol), **D^{0}C$_6$D^0** (2.95 g, 10.20 mmol), 5 mL of methanol, 500 μL of water, and 500 μL (0.1 m) of hydrochloric acid was sol–gel processed: yield 2.65 g (89.8%); ^{13}C CP/MAS NMR 49.6 ($SiOCH_3$), 33.4 ($Si(CH_2)_2$-$CH_2CH_2(CH_2)_2Si$), 23.2 ($SiCH_2CH_2(CH_2)_2CH_2CH_2Si$), 17.7 ($SiCH_2(CH_2)_4CH_2Si$), −0.1 ($SiCH_3$); ^{29}Si CP/MAS NMR (silicon substructure) −9.7, −13.3 (D^1), −22.2 (D^2). Anal. Calcd for $C_{19}H_{21}O_{1.5}Si(C_8H_{18}O_2Si_2)_{10000}$: C, 47.48; H, 8.96. Found: C, 47.19; H, 8.82%. BET surface $A_{BET}=3.68\ m^2\ g^{-1}$.

2.1.6. Preparation of the polysiloxane 2(T^n)(T^{m}C$_6$T^m)$_y$. A mixture of **2(T^0)** (0.8 mg, 2.16×10^{-3} mmol), **T^{0}C$_6$T^0** (3.37 g, 10.30 mmol), 5 mL of methanol, 500 μL of water, and 500 μL (0.1 mol) of ammonia was sol–gel processed: yield 3.25 g (96.4%); ^{13}C CP/MAS NMR 49.8 ($SiOCH_3$), 33.1 ($Si(CH_2)_2$-$CH_2CH_2(CH_2)_2Si$), 23.0 ($SiCH_2CH_2(CH_2)_2CH_2CH_2Si$), 11.4 ($SiCH_2(CH_2)_4CH_2Si$); ^{29}Si CP/MAS NMR (silicon substructure) −41.7 (T^0), −49.9 (T^1), −58.7 (T^2), −67.4 (T^3). Anal. Calcd for $C_{19}H_{21}O_{1.5}Si(C_6H_{12}O_3Si_2)_{10000}$: C, 41.82; H 7.02. Found: C, 40.46; H, 6.85%. BET surface $A_{BET}=63.0\ m^2\ g^{-1}$.

2.2. Fluorescence measurements

All measurements on the hybrid polymers were obtained by suspending 3–4 mg of the powders in 3 mL of solvent and vigorously stirring the samples with a magnetic stirrer to avoid sedimentation. The temperature during the measurements was kept constant at $T=293$ K. For exciplex experiments, 0.5–1.5 mL of freshly distilled triethylamine were added to the liquid phase. Fluorescence depolarisation by light scattering has not been observed at the concentrations of polymeric material in the liquid phase used in the present study. Also, fluorescence depolarisation by energy transfer between fluorene moieties did not occur. At the employed molar ratio of 10^{-4} between **2(T^0)** and co-condensation agents, corresponding to a local concentration of fluorene in the polysiloxane matrix of $c\approx4\times10^{-4}$, the mean distance between two fluorene molecules of $\bar{R}=16$ nm is much larger than the critical distance of $R_C=2.2$ nm calculated for homo transfer between fluorene molecules. This consideration is confirmed by experiment. The observed values of fluorescence anisotropy for local concentrations of fluorene of $c\approx4\times10^{-4}$ M and $c\approx4\times10^{-5}$ M are identical within experimental error.

Steady-state fluorescence, fluorescence excitation, and fluorescence anisotropy spectra were obtained on a SPEX Fluorolog 222 fluorometer, equipped with Glan–Thompson polarisers.

Fluorescence and fluorescence anisotropy decay curves were acquired by the single-photon counting method. Where nanosecond time-resolution was sufficient, a thyratron-controlled hydrogen/nitrogen flashlamp (Photochemical Research Associates, Model 510B) was used for excitation and a R928 photomultiplier tube (Hamamatsu) for detection. The signal from the photomultiplier tube was fed into a multichannel analyzer *via* a picosecond amplifier/discriminator and a time to amplitude converter (EG&G ORTEC). The time resolution of this setup is limited to $\Delta t=0.5$ ns.

Where picosecond time resolution was required, the instrument for time-domain fluorescence experiments at the "Center for Fluorescence spectroscopy", Baltimore, MD, USA, was used. It comprised a frequency doubled rhodamine dye laser synchronously pumped by a mode-locked argon ion laser. The laser system provided trains of 290 nm light pulses at a repetition frequency of 3.77 MHz and a pulsewidth of about 7 ps FWHM. The collected fluorescence light passed through a polariser, low-pass filter, and monochromator and was detected by a MCP photomultiplier (Hamamatsu). The time-correlated single photon counting detection system was based on standard NIM modules purchased from EG&G Ortec or Tennelec, and Norland 5700 MCA. The impulse response function of the instrument had a width of 70 ps FWHM. The time resolution was comparable with the width of the response function for experiments analyzed by a direct fitting of the experimental data without deconvolution.

The experimental unpolarised fluorescence decay curves, $I(t)$, were fitted to sums of n exponentials ($n=1$–3), $I(t)=\sum_{i=1}^{n}A_i e^{-t/\tau_i}$. The quality of the fit was assessed by the values of χ^2 and the Durbin–Watson parameter, as well as from the plots of residuals and autocorrelation functions. Fits obtained with $n+1$ exponentials were preferred to those with n exponentials only if χ^2 was reduced significantly. The mean fluorescence decay times were calculated by

$$\langle\tau_F\rangle=\sum_{i=1}^{n}A_i\tau_i^2/\sum_{i=1}^{n}A_i\tau_i \quad (1)$$

Anisotropy decay curves, $r(t)$, were obtained from polarised fluorescence decay curves $I_{vv}(t)$ and $I_{vh}(t)$

$$r(t)=\frac{I_{vv}(t)-gI_{vh}(t)}{I_{vv}(t)+2gI_{vh}(t)}, \quad (2)$$

where $g=I_{hv}/I_{hh}$ accounts for the polarisation dependent sensitivity of the detection system. All polarised decay curves were recorded with picosecond time resolution. The $r(t)$ curves were also fitted to sums of exponentials, allowing for constant offsets. Steady state anisotropies, r_{ss}, were obtained with the corresponding steady state fluorescence intensities.

3. Results

3.1. Synthesis of the T-silyl functionalised fluorene 2(T^0)

To bind fluorene in the 9-position to a hydrocarbon spacer with a terminal T-silyl function, it is derivatised with butyllithium to the corresponding lithium compound (Scheme 1). Subsequently

there follows a coupling reaction with 1-bromohex-5-ene to give the unsaturated intermediate **1**.[35] In the presence of H_2PtCl_6 as catalyst a hydrosilylation reaction takes place between **1** and $HSiCl_3$ to give the trichlorosilane **2** which is immediately transformed to **2(T^0)** with trimethyl orthoformate. After column chromatographic purification **2(T^0)** is a yellow oil which is sensitive to moisture and dissolves readily in organic solvents of medium polarity. The composition of **2(T^0)** was verified by its EI mass spectrum showing the expected molecular peak. Analytical data are summarised in the Experimental section.

3.2. Synthesis of the polymeric fluorenes

Stationary phases containing fluorene have to be investigated by fluorescence spectroscopy in a highly diluted form. Therefore the sol–gel process of **2(T^0)** was carried out in the presence of high amounts ($1:10^4$) of the mono- and bifunctional co-condensation agents **MeT^0**, **T^{0}C$_6$T^0**, and **D^{0}C$_6$D^0** (Scheme 2) influencing the properties of the resulting polymeric materials essentially. For reasons of comparison also the fluorene **2(T^0)** without any co-condensation agent was subjected to a sol–gel procedure. The properties of sol–gel processed materials strongly depend on the applied reaction conditions such as concentration of the starting materials, amount and type of solvent, temperature, reaction time, drying conditions of the wet gel, and type of catalyst. To ensure the same reaction kinetics for the synthesis of each polymer as a prerequisite for comparable results, the adherence to uniform reaction conditions has to be maintained during the entire hydrolysis and polycondensation procedure.[4,35–37] Methanol was added during the sol–gel process to homogenise the reaction mixture. Ammonia [**2(T^n)**, **2(T^n)(MeT^m)$_y$**, **2(T^n)(T^{m}C$_6$T^m)**] and hydrogen chloride [**(2T^n)(D^{i}C$_6$D^i)$_y$**] were appropriate catalysts, which do not interfere with fluorene.[38]

The ^{1}H and ^{13}C{^{1}H} NMR spectra of the polymer **2(T^n)** (suspension in $CDCl_3$) reveal broadened ^{1}H and ^{13}C resonances, respectively. However, the pattern of these ^{1}H and ^{13}C signals is similar to that of the respective high resolution ^{1}H and ^{13}C{^{1}H} NMR spectra of the monomeric precursor **2(T^0)** which is evidence that fluorene remained intact during the sol–gel process.

The ^{29}Si and ^{13}C CP/MAS NMR spectra of the polymeric materials **2(T^n)(MeT^m)$_y$**, **2(T^n)(D^{i}C$_6$D^i)$_y$**, and **2(T^n)-(T^{m}C$_6$T^m)$_y$** ($y=10^4$) are dominated by the polymeric parts **MeT^m**, **D^{i}C$_6$D^i**, and **T^{m}C$_6$T^m**. Hence no ^{29}Si signals for the T^n functions of **2(T^n)** are observed. The ^{29}Si CP/MAS NMR spectrum of **2(T^n)(MeT^m)$_y$** is characterised by two resonances of different intensity which are assigned to T^2 (small) and T^3 (intensive) silyl species. In the case of **2(T^n)(D^{i}C$_6$D^i)$_y$** two signals are observed for D^1 silyl groups, probably because of diastereotopic effects. An intense signal occurs for the completely hydrolyzed D^2 functions. The ^{29}Si CP/MAS NMR spectrum of **2(T^n)(T^{m}C$_6$T^m)$_y$** shows all resonances for T^0- ,T^1- ,T^2-, and T^3-silyl groups. Obviously also noncrosslinked T-silyl species are present in the polymer. Both spectra are similar to those of the pure hybrid polymers **D^{i}C$_6$D^i** and **T^{m}C$_6$T^m** which were reported recently.[6,38] The ^{13}C CP/MAS NMR spectra of the stationary phases **2(T^n)(MeT^m)$_y$**, **2(T^n)(D^{i}C$_6$D^i)$_y$**, and **2(T^n)(T^{m}C$_6$T^m)$_y$** show resonances at δ 50.0 which are attributed to the carbon atoms of silicon bound methoxy groups. This is consistent with an incomplete hydrolysis and thus a reduced crosslinkage of the polymers. Because of steric effects the fraction of nonhydrolyzed methoxy residues is higher in the case of the polymer **2(T^n)(T^{m}C$_6$T^m)$_y$**. However, the concentration of residual methoxy groups is rather small, because hydrolysis and condensation of the materials must be fairly complete as is obvious from the similarity of experimental elemental analysis data and the values calculated for fully reacted materials.

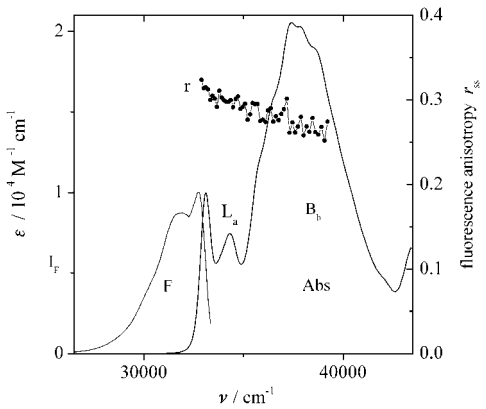

Fig. 1 Absorption (Abs), fluorescence (F) and fluorescence anisotropy spectra (r) of **2(T^0)** in PMMA glass.

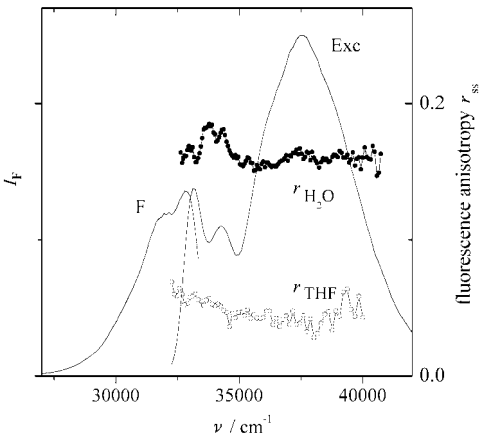

Fig. 2 Fluorescence and fluorescence excitation spectra of **2(T^n)(D^i-C$_6$-D^i)$_y$** in THF as well as the anisotropy spectra of **2(T^n)(D^i-C$_6$-D^i)$_y$** in water and in THF. The maximum at 34000 cm^{-1} in the anisotropy spectrum in water is due to the Raman peak of water.

3.3. Fluorescence spectroscopic investigations

3.3.1. Fluorescence and fluorescence excitation spectra of 2(T^0). Fig. 1 presents the UV/Vis absorption and fluorescence spectra of **2(T^0)** in solution. The vibrationally structured low-energetic absorption band is assigned to the A→L$_a$ transition,[39] while the strong and structureless absorption band at 38500 cm^{-1} is assigned to the A→B$_b$ transition.[39] Upon binding **2(T^0)** to the hybrid polysiloxanes, fluorescence and fluorescence excitation spectra do not change noticeably (see Fig. 2). No aggregation of the fluorophores is observable in the spectra.

3.3.2. Fluorescence decay curves of 2(T^0). The fluorescence decay curves of **2(T^0)** dissolved homogeneously in low viscosity solutions are single exponential with decay times of $\tau_F \approx 6$ ns (Table 1). Only in dichloromethane, the fluorescence lifetime is

Table 1 Mean fluorescence decay time $\langle\tau_F\rangle$ of 2(T^0) in homogeneous solutions and of the polysiloxane hybrid polymers suspended in different liquids

$\langle\tau_F\rangle$/ns	Cyclohexane	THF	Dichloromethane	Methanol
Solution[a]	6.4	6.0	3.6	6.5
2(T^n)(MeT^m)$_y$[b]	6.0	5.3	4.0	6.2
2(T^n)(D^{i}C$_6$D^i)$_y$[b]	6.0	5.6	4.3	6.2
2(T^n)(T^{m}C$_6$T^m)$_y$[b]	6.0	5.5	4.2	6.2

[a]The values in solution are obtained from exponential fits to the decay curves. [b]The values in the polysiloxane matrices are calculated by eqn. (1), inserting the data obtained from biexponential fits.

reduced to $\tau_F \approx 3$ ns, indicating that this liquid partially quenches the excited singlet state of **2(T^0)**, due to the heavy atom effect of chlorine. For suspensions of the fluorene-labeled polysiloxanes in all investigated solvents, slightly nonexponential decay curves are observed. This type of decay curve is best described by narrow distributions of decay times, but can also be fitted by sums of two exponentials without loss of accuracy. The deviation from exponentiality implies that the fluctuations of the microenvironment of the fluorophores are slow on the time scale of fluorene fluorescence. The mean fluorescence decay times of the fluorene labeled polymer suspended in, *e.g.*, cyclohexane, THF, and methanol are close to the values obtained for the corresponding homogeneous solutions of **2(T^0)** (Table 1). The decay curves of suspensions of the polymers in dichloromethane show two clearly distinct lifetime components of $\tau_F \approx 5$ ns and $\tau_F \approx 3$ ns of about equal weight, which result in mean decay times which are significantly longer than those of **2(T^0)** in dichloromethane solution (Table 1). The existence of the long lifetime component indicates that a considerable fraction of the matrix bound probes is quenched less than in bulk solution, and thus is partly protected from dichloromethane by the matrix.[40,41]

3.3.3. Steady state measurements of fluorescence anisotropy. Fluorene, for which R = H (see Scheme 1), belongs to the point group C_{2v}, and both of the transitions corresponding to the L_b- and B_b-bands are of $A_1 \rightarrow B_2$ type in terms of symmetry. Hence, the transitions are polarised along the molecular *y*-axis.[42,30] Upon introduction of an alkyl group for R, as in **2(T^0)**, the local symmetry of the π-electron system is hardly affected and consequently the orientation of the transition dipole moments remains practically unchanged. The fluorescence anisotropy excitation spectrum of **2(T^0)** embedded in a rigid poly(methyl methacrylate) (PMMA) resin (Fig. 1) shows a steady-state anisotropy of $r_0 \approx 0.30$ for the lowest energy transition. The steady state fluorescence anisotropy decreases with decreasing excitation wavelength due to increased light scattering by the PMMA matrix.

In homogeneous solutions of **2(T^0)** in low viscosity solvents, the steady state fluorescence anisotropy, r_{ss}, is not significantly different from zero. Upon binding **2(T^0)** to the polymer matrix, much higher values of r_{SS} are obtained. In Fig. 2, the fluorescence anisotropy excitation spectra of **2(T^n)(D^{i}C$_6$D^i)$_y$** in THF and water are shown as typical examples. By inserting *r* into eqn. (3)

$$\langle \tau_R \rangle \approx \frac{\langle \tau_F \rangle}{\frac{r_0}{r_{ss}} - 1} \qquad (3)$$

which is valid for small deviations of fluorescence decay curves from exponentiality, the mean rotational correlation time, $\langle \tau_R \rangle$, is obtained. As the mean fluorescence decay times, $\langle \tau_F \rangle$, are similar for all solvents (except for dichloromethane), the steady-state values of *r* already give a rough measure of the mobility of the probe. The values of $\langle \tau_R \rangle$ for matrix bound **2(T^n)**, calculated by eqn. (1), are about one to two orders of magnitude larger than the value of $\langle \tau_R \rangle \approx 30$ ps, obtained for fluorene in solution (Table 2). A more detailed picture of the microenvironment of the probe can be obtained by time-resolved measurements of the fluorescence anisotropy.

3.3.4. Time resolved measurements of fluorescence anisotropy. Fig. 3 shows typical decay traces of fluorescence anisotropy after pulsed laser excitation of the samples. The fluorescence anisotropy decay of fluorene dissolved in THF is faster than the instrument response time of $\tau = 70$ ps. For matrix bound **2(T^n)**, strongly nonexponential fluorescence anisotropy decay curves are obtained. Fitting them to sums of three exponentials yields correlation times, which fall into three distinctly different time ranges, namely $\tau_{R1} = 100$–200 ps, $\tau_{R2} = 1$–3 ns, and $\tau_{R3} = 10$–50 ns. No residual anisotropies are obtained from fitting the decay curves in the accessible time range ($0 \text{ ns} < t < 15$ ns). Even the fastest component, τ_{R1}, is significantly slower than the anisotropy decay of fluorene in homogeneous solution, due to the reduced mobility of the probe molecules. The mobility is affected by both the type of the polysiloxane matrix and the liquid in which the polymer is

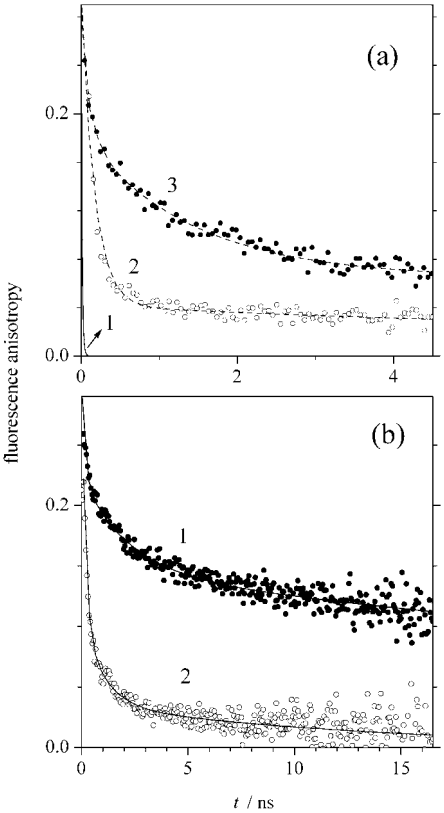

Fig. 3 Theoretical fluorescence anisotropy decay curve of fluorene in THF (curve 1 in Fig. 3a), calculated from the data of ref. 33 by eqn. (2), and examples of experimental fluorescence anisotropy decay traces after pulsed laser excitation ($\lambda_{ex} = 295$ nm, $\Delta t = 10$ ps fwhm). (a) **2(T^n)(T^m-C$_6$-T^m)$_x$** (2) and **2(T^n)(D^i-C$_6$-D^i)$_y$** (3) suspended in THF. (b) **2(T^n)(Me-T^m)$_y$** suspended in cyclohexane (1) and in dichloromethane (2). Points: experimental data, lines: three-exponential fits.

Table 2 Steady state fluorescence anisotropies, r_{ss}, and mean rotational correlation times, $\langle \tau_R \rangle$, in italics, of fluorene-labeled polysiloxane hybrid polymers suspended in different liquids

$\langle \tau_R \rangle$/ns		Cyclohexane	Diethyl ether	THF	Dichloromethane	Methanol	Water
2(T^n)(MeT^m)$_y$	r_{ss}	0.14	0.005	0.005	0.025	0.06	0.12
	$\langle \tau_R \rangle$/ns[a]	*3.8*	*0.07*	*0.08*	*0.30*	*1.20*	*3.20*
2(T^n)(D^{i}C$_6$D^i)$_y$	r_{ss}	0.14	0.045	0.045	0.08	0.13	0.16
	$\langle \tau_R \rangle$/ns[a]	*3.8*	*0.90*	*0.80*	*1.20*	*3.50*	*4.50*
2(T^n)(T^{m}C$_6$T^m)$_y$	r_{ss}	0.06	0.025	0.02	0.025	0.06	0.11
	$\langle \tau_R \rangle$/ns[a]	*1.2*	*0.45*	*0.30*	*0.30*	*1.20*	*2.80*

[a]The values of $\langle \tau_R \rangle$ are calculated by eqn. (3) from steady state fluorescence anisotropies, r_{ss}, and mean fluorescence decay times, $\langle \tau_F \rangle$.

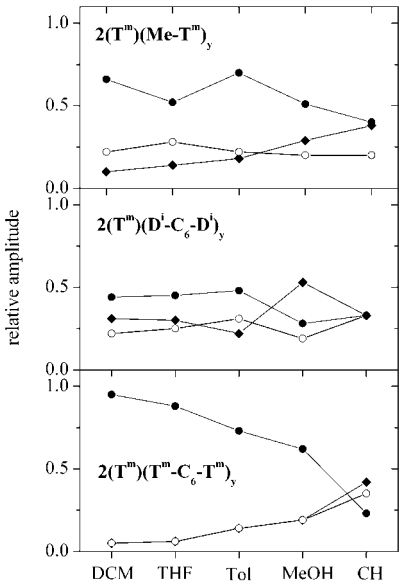

Fig. 4 Relative amplitudes of the three components of the fluorescence anisotropy decays for the hybrid polymers in different liquids. Points: short component ($\tau_{R1}=0.1$–0.2 ns), open circles: medium component ($\tau_{R2}=1.0$–3.0 ns), diamonds: long component ($\tau_{R3}=10$–50 ns). DCM: dichloromethane, THF: tetrahydrofuran, Tol: toluene, MeOH: methanol, and CH: cyclohexane.

suspended. Fig. 4 gives a graphic representation of the amplitudes of the three components of τ_R for the three polymers suspended in different liquids. For **2(T^n)(T^{m}C$_6$T^m)$_y$**, a clear trend of the amplitudes with the suspending solvent is observable. In dichloromethane and in THF the short component, τ_{R1}, is dominating, indicating a high mobility of the fluorophore. In cyclohexane, almost no contribution of the short component is left, which is due to strongly hindered motions of the probe molecule. In **2(T^n)(D^{i}C$_6$D^i)$_y$**, the contribution of the short component is small in all solvents, corresponding to solvent independent low mobility of the fluorophore. In the case of **2(T^n)(MeT^m)$_y$**, an intermediate situation is found.

3.3.5. Investigation of the translational mobility by exciplex formation between triethylamine and fluorene in 2(T^n). The translational mobility of low molecular weight species dissolved in the mobile component is available from the analysis of bimolecular processes such as exciplex formation. Upon electronic excitation, fluorene forms an exciplex with triethylamine (TEA).[43] This also holds true for fluorene in **2(T^n)**. These exciplexes exhibit structureless fluorescence spectra (Fig. 5), which are red-shifted against the emission of molecular fluorene. The spectral position of the exciplex band shifts to longer wavelengths with increasing polarity of the environment, due to the large dipole moment of the exciplex of $\mu=13$ D.[43] In homogeneous solutions of fluorene in mixtures of TEA and *n*-hexane, the maximum of the exciplex emission is found at $\tilde{\nu}\approx26000$ cm^{-1}. In suspensions of **2(T^n)(D^{i}C$_6$D^i)$_y$** in THF–TEA mixtures, the emission maximum is shifted to $\tilde{\nu}\approx23000$ cm^{-1}, indicating that the exciplex is at least partially solvated by THF.

For suspensions of the hybrid polymers in dichloromethane, THF, diethyl ether, and toluene sufficient amounts of exciplex are formed, whereas in methanol and cyclohexane no significant exciplex formation is observed. Fig. 6 shows the fluorescence decay curves of a suspension of **2(T^n)(D^{i}C$_6$D^i)$_y$** in a diethyl ether–TEA mixture. In this example, the mean fluorescence decay time of **2(T^n)** is reduced to $\bar{\tau}_F=4.5$ ns, against $\bar{\tau}_F=6.0$ ns before addition of TEA. The time-resolved intensity trace of the exciplex fluorescence reveals two rising

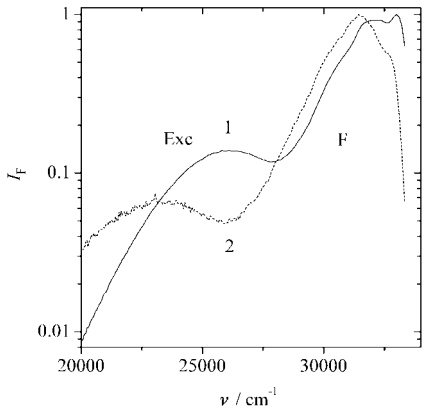

Fig. 5 Fluorescence spectra of the system fluorene–triethylamine (TEA). (1) solution of fluorene (10^{-5} M) and TEA (0.1 M) in *n*-hexane. (2) Suspension of **2(T^n)(D^i-C$_6$-D^i)$_y$** in 1 M solution of TEA in THF. Excitation wavelength $\lambda_{ex}=280$ nm. F: Fluorene fluorescence, Exc: Exciplex fluorescence.

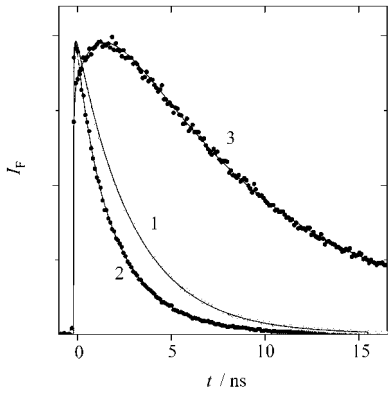

Fig. 6 Fluorescence decay curves of suspensions of **2(T^n)(D^i-C$_6$-D^i)$_y$** in diethyl ether after pulsed laser excitation (laser pulse width $\Delta t=10$ ps fwhm). (1) fluorene fluorescence without TEA. (2) fluorene fluorescence for $c_{TEA}=1$ M. (3) exciplex fluorescence for $c_{TEA}=1$ M. Excitation wavelength $\lambda=290$ nm, detection of fluorene and exciplex fluorescence at $\lambda=340$ nm and $\lambda=410$ nm, respectively.

components, one of which is instantaneous on the time scale of our experiment. The instantaneous component is due to "static" exciplexes, which are formed upon excitation of ground state aggregates of **2(T^n)** and TEA. The slow rising component has a rise time of $\tau_F=3.5$ ns. Considering the inhomogeneity of the sample and the nonexponentiality of the decay traces, this rise time may be regarded as being approximately equal to the decay time of **2(T^n)** and is thus ascribed to the dynamic formation of the exciplex. The decaying component of the exciplex trace, with $\tau_F=16.3$ ns, is assigned to the deactivation of the exciplex to the ground state complex.

4. Discussion

4.1. Rotational mobility of fluorene and 2(T^n)

In the case of fluorene in bulk solutions, *i.e.* R=H (see Scheme 1), fluorescence will be depolarised by rotational diffusion around the principal *x*- and *z*-axes, as the transition dipole moment of emission is oriented parallel to the principal *y*-axis of rotation to a good approximation. These two diffusional motions result in a biexponential decay of the fluorescence anisotropy[44]

$$r(t) = \frac{1}{5}\left[1 + \frac{2D_y - D_x - D_z}{2\Delta}\right] e^{-(6\bar{D}-2\Delta)t} + \frac{1}{5}\left[1 - \frac{2D_y - D_x - D_z}{2\Delta}\right] e^{-(6\bar{D}+2\Delta)t} = A_1 e^{-t/\tau_{R1}} + A_2 e^{-t/\tau_{R2}} \quad (4)$$

where $\bar{D} = \frac{D_x + D_y + D_z}{3}$ and $\Delta = \sqrt{D_x^2 + D_y^2 + D_z^2 - D_x D_y - D_y D_z - D_z D_x}$ The rotational diffusion constants of fluorene in $CDCl_3$ at $T = 310$ K have been determined by T_1 relaxation measurements of ^{13}C NMR signals as $D_x = 2.8 \times 10^{10}$ s^{-1}, $D_y = 2.1 \times 10^{10}$ s^{-1}, and $D_z = 0.73 \times 10^{10}$ s^{-1}.[45] These values are in agreement with results obtained by depolarised Raman scattering, which yield $C = 27$ ps (mPa s)$^{-1}$ for the viscosity dependent part of the rotational correlation time, $\tau_R = C + \tau_0$.[46] Inserting the diffusion constants D_x, D_y, and D_z into eqn. (4) yields the theoretical fluorescence anisotropy decay curve of fluorene in $CDCl_3$ shown in Fig. 3a. The rotational correlation times and their respective amplitudes are calculated as $\tau_{R1} = 13.4$ ps ($A_1 = 0.24$) and $\tau_{R2} = 6.8$ ps ($A_2 = 0.16$). Very similar parameters are expected for fluorene in THF at $T = 293$ K, because the viscosity of THF at $T = 293$ K ($\eta = 0.48$ mPa s) is practically identical to that of $CHCl_3$ at $T = 310$ K ($\eta = 0.47$ mPa s).[47] Thus, the theoretical decay curve of fluorene in THF cannot be obtained experimentally with our setup, due to its limited time resolution.

When the fluorophore is attached to the hybrid polymer matrix, the mobility of the fluorene moiety is strongly reduced by the alkyl spacer and by the geometry of the environment, resulting in slow and strongly nonexponential fluorescence anisotropy decay curves. Although the inhomogeneity of the environment leads to a broad distribution of rotational correlation times, three significantly different ranges of correlation times are obtained, which can tentatively be assigned to characteristic motions of the fluorophore. Each of these motions may be associated with a specific site of the probe molecules.[8] The short correlation time component of $\tau_R = 100$–200 ps is ascribed to fast, practically unimpeded motions of the fluorophore. The most important of these motions is fast rotation of the fluorene moiety around the C_9–C_{10}-bond of the alkyl spacer (see Schemes 1 and 2). This motion is only weakly hindered if the pores in the polymer matrix are large compared to the fluorophore size. According to eqn. (4) and similar treatments described in refs. 48–50 this rotation leads to a single exponential decay

$$r(t) = 0.1 + 0.3e^{-4D_z' t} \quad (5)$$

which does not decay to zero, even for infinitely long times after the laser pulse. The diffusion coefficient, D_z', for rotation around the C_9–C_{10} bond, adopts values in the range 0.6×10^9 s$^{-1} \leqslant D_z' \leqslant 2.5 \times 10^9$ s^{-1}. Motions of larger segments of the alkyl spacers, with correlation times in the medium time range of 1–3 ns, eventually lead to complete depolarisation, because they make the whole solid angle accessible to the transition dipole moment. As these motions involve different conformations of the alkyl spacers, they require relatively large free volumes. The long correlation time components of $\tau_R > 10$ ns comprise motions which are slow compared to the fluorescence lifetime of **2(T^n)** of $\tau_F \approx 5$–6 ns and correspond to almost complete immobilisation of the fluorophore caused by very small free volumes or strongly attractive interactions between **2(T^n)** and the polymeric backbone.

4.2. Translational mobility of 2(T^n) and TEA

For suspensions of the hybrid polymers in dichloromethane and diethyl ether the rate constants of formation; k_{MD}, of the exciplexes are calculated by means of eqn. (6) from the dynamic portion of the quenching of fluorene fluorescence

$$k_{MD} = \left(\frac{1}{\tau_F} - \frac{1}{\tau_F^0}\right)\frac{1}{c_{TEA}} \quad (6)$$

where τ_F and τ_F^0 are the fluorescence decay times of fluorene at the given concentration of TEA, c_{TEA}, and without TEA, respectively. The results summarised in Table 3 are obtained under the assumption that the concentration of TEA in the polymer is the same as in the bulk solution. They must be considered as mean values, from which considerable deviations may occur in different regions of the polymer.[8] The rate constants, k_{MD}, in the interphases are reduced by an order of magnitude against the values in homogeneous solutions. The latter are known to be close to the diffusion limit, *e.g.*, $k_{MD} = 1.1 \times 10^9$ M^{-1} s^{-1} has been obtained in cyclohexane.[43] It is thus inferred that the translational mobility in the three hybrid polymers under investigation is greatly reduced compared to that observed in bulk solution. The translational mobility decreases by a factor of two in the series **2(T^n)(MeT^m)$_y$** $\geqslant$ **2(T^n)(T^{m}C$_6$T^m)$_y$** $>$ **2(T^n)(D^{i}C$_6$D^i)$_y$** (Table 3).

5. Conclusion

The fluorescence spectroscopic investigations of rotational and translational mobility in organic–inorganic hybrid polymers show clearly that both the rotational mobility of the matrix bound active centers and the translational mobility of low molecular weight species dissolved in the liquid phase are reduced by one to two orders of magnitude compared to homogeneous solutions. Obviously, diffusion processes in the interphase are appreciably hindered by the polymer matrix. This observation is in agreement with the small swelling volumes of the polymers in liquids. The largest diffusion coefficients are obtained in dichloromethane, THF and diethyl ether, in which the swelling volumes reach almost 10% of the original volumes. In all other solvents, in which no swelling of the polymers is measurable, the diffusion coefficients are significantly smaller. In polar liquids, the mobility of the probe molecules is further reduced due to their low solubility in these solvents, which leads to adsorption of the probe molecules to the polymer backbone.

In all liquids, the translational and rotational diffusion coefficients found in **2(T^n)(T^{m}C$_6$T^m)$_y$** and **2(T^n)(MeT^m)$_y$** are significantly larger than those obtained in **2(T^n)(D^{i}C$_6$D^i)$_y$**. As swelling does not substantially increase the free volumes of the materials, this dependence of mobility on the type of material is probably due to the inherently larger pore volumes of materials based on co-condensation agents with T-silyl groups compared to those built from co-condensation agents carrying D-silyl groups. It is known that in materials which are prepared from monomers with D-silyl functions less rigid pore structures are formed than in materials consisting of monomers with T-silyl functions. Actually, the BET surface area for **2(T^n)(T^{m}C$_6$T^m)$_y$** exceeds that of **2(T^n)(D^{i}C$_6$D^i)$_y$** by a factor of almost twenty. However, the extremely small BET surface area found for **2(T^n)(MeT^m)$_y$** does not fit into this concept. The nonpolar nature of **2(T^n)** may offer a possible explanation for the high mobilities observed in both T-silyl based materials compared to

Table 3 Rate constants k_{MD} of exciplex formation between 2(T^n) and triethylamine in the hybrid polymers, suspended in dichloromethane and in diethyl ether[a]

Polymer	In dichloromethane $k_{MD}/10^8$ M^{-1} s^{-1}	In diethyl ether $k_{MD}/10^8$ M^{-1} s^{-1}
2(T^n)(MeT^m)$_y$	2.4	2.3
2(T^n)(D^{0}C$_6$D^0)$_y$	1.4	1.1
2(T^n)(T^{0}C$_6$T^0)$_y$	2.1	1.8

[a]The values of k_{MD} are calculated by eqn. (6).

those found in the D-silyl based polymer. The relatively polar silanes, mainly those with T-silyl functions, tend to avoid the vicinity of **2(T″)** during the sol–gel process, thus forming pores large enough to allow unimpeded diffusional motions of the fluorene moiety. As D-silyl functions do not form rigid pore structures, only pores formed by T-silyl moieties are persistent. The pores caused by this template effect[39,40] do not show up in the BET measurements because the mole fraction of **2(T″)** is only 10^{-4}.

In order to reach the goal of combining high chemical stability of the interphases with solution-like accessibility of the active centers, the swelling capability of the polysiloxane backbone has to be improved appreciably, *e.g.* by introducing phenyl groups into the organic parts of the cocondensation agents. An alternative approach is the synthesis of highly micro- or mesoporous materials, making use of the template effect.[51,52]

Acknowledgements

We thank J. R. Lakowicz for giving us access to the Center for Fluorescence Spectroscopy, University of Maryland at Baltimore, U.S.A. We are also grateful to P. C. Schmidt and A. Brenn for providing us with BET-measurements on the hybrid polymers. Thanks are also due to W. Wielandt for his help with the synthesis and S. Brugger for the NMR measurements. The support of this research by the Deutsche Forschungsgemeinschaft (Forschergruppe, Grant FOR 184/3-1, and Graduiertenkolleg, Grant GK-GRK 441/1-00), Bonn/Bad Godesberg, and by the Fonds der Chemischen Industrie, Frankfurt/Main, is gratefully acknowledged.

References

1 Supported Organometallic Complexes. Part 22. Part 21: E. Lindner, T. Salesch, F. Höhn and H. A. Mayer, *Z. Anorg. Allg. Chem.*, 1999, **625**, 2133.
2 M. T. Murtagh, M. R. Shariari and M. Krihak, *Chem. Mater.*, 1998, **10**, 3862.
3 M. A. Chan, J. L. Lawless, S. K. Lam and D. Lo, *Anal. Chim. Acta*, 2000, **408**, 33.
4 E. Lindner, F. Auer, T. Schneller and H. A. Mayer, *Angew. Chem., Int. Ed.*, 1999, **38**, 2154.
5 J. H. Clark and D. J. Mcquarrie, *Chem. Soc. Rev.*, 1996, **96**, 303.
6 E. Lindner, T. Schneller, H. A. Mayer, H. Bertagnolli, T. S. Ertel and W. Hörner, *Chem. Mater.*, 1997, **9**, 1524.
7 E. Lindner, R. Schreiber, M. Kemmler, T. Schneller and H. A. Mayer, *Chem. Mater.*, 1995, **7**, 951.
8 B. Dunn and J. I. Zink, *Chem. Mater.*, 1997, **9**, 2281.
9 M. A. Meneses-Nava, O. Barbosa-Garcia, L. A. Diaz-Torres, S. Chavez-Cerda and T. A. King, *Opt. Mater.*, 1999, **13**, 327.
10 K. Maruszewski, M. Jasiorski, M. Salamon and W. Strek, *Chem. Phys. Lett.*, 1999, **314**, 83.
11 P. Innocenzi, H. Kozuka and T. Yoko, *J. Phys. Chem. B*, 1997, **101**, 2285.
12 G. Hungerford, K. Suhling and J. A. Ferreira, *J. Photochem. Photobiol. A*, 1999, **129**, 71.
13 I. M. Ilharco and J. M. G. Martinho, *Langmuir*, 1999, **15**, 7490.
14 K. K. Flora, M. A. Dabrowski, S. P. Musson and J. D. Brennan, *Can. J. Chem. Rev. Can. Chim.*, 1999, **77**, 1617.
15 C. D. Geddes, J. M. Chevers and D. J. S. Birch, *J. Fluorescence*, 1999, **9**, 73.
16 A. C. Franville, D. Zambon, R. Mahiou and Y. Troin, *Chem. Mater.*, 2000, **12**, 428.
17 Y. W. Hou, A. M. Bardo, C. Martinez and D. A. Higgins, *J. Phys. Chem. B*, 2000, **104**, 212.
18 M. H. Huang, H. M. Soyez, B. S. Dunn and J. I. Zink, *Chem. Mater.*, 2000, **12**, 231.
19 S. M. Arabei, T. A. Pavich, J. P. Galaup and P. Jardon, *Chem. Phys. Lett.*, 1999, **306**, 303.
20 D. S. Gottfried, A. Kagan, B. M. Hoffman and J. M. Friedman, *J. Phys. Chem. B*, 1999, **103**, 2803.
21 J. L. H. Jiwan, E. Robert and J. P. Soumillion, *J. Photochem. Photobiol. A*, 1999, **122**, 61.
22 U. Narang, R. A. Dunbar, F. V. Bright and P. N. Prasad, *Appl. Spectrosc.*, 1993, **47**, 1700.
23 R. C. Chambers, Y. Haruvy and M. A. Fox, *Chem. Mater.*, 1994, **6**, 1351.
24 P. B. Leezenberg, M. D. Fayer and C. W. Frank, *Pure Appl. Chem.*, 1996, **68**, 1381.
25 T. Suratwala, Z. Gardlund, K. Davidson and D. R. Uhlmann, *Chem. Mater.*, 1998, **10**, 190–198.
26 J.-L. Habib Jiwan, E. Robert and J.-Ph. Soumillion, *J. Photochem. Photobiol. A*, 1996, **122**, 61–68.
27 N. Leventis and I. A. Elder, *Chem. Mater.*, 1999, **11**, 2837.
28 Ch. Malins, S. Fanni, H. G. Glever, J. G. Vos and B. D. MacCraith, *Anal. Commun.*, 1999, **36**, 3.
29 A. H. O. Karkkainen, O. E. O. Hormi and J. T. Rantala, *Proc. SPIE – Int. Soc. Opt. Eng.*, 2000, **3943**, 194.
30 J. C. Biazzotto, H. C. Sacco, K. J. Ciuffi, C. R. Neri, A. G. Ferreira, Y. Iamamoto and O. A. Serra, *J. Non-Cryst. Solids*, 1999, **247**, 134.
31 A. Lobnik, I. Oehme, I. Murkovic and O. S. Wolfbeis, *Anal. Chim. Acta*, 1998, **367**, 159.
32 T. Ishikawa, H. Inoue and A. Makishima, *J. Non-Cryst. Solids*, 1996, **203**, 43.
33 R. J. P. Corriu, P. Hesemann and G. F. Lanneau, *Chem. Commun.*, 1996, 1845.
34 M. Plaschke, R. Czolk, J. Reichert and H. J. Ache, *Thin Solid Films*, 1996, **279**, 233.
35 W. Wielandt, A. Ellwanger, K. Albert and E. Lindner, *J. Chromatogr. A*, 1998, **805**, 71.
36 L. L. Hench and J. K. West, *Chem. Rev.*, 1990, **90**, 33.
37 D. A. Loy and K. J. Shea, *Chem. Rev.*, 1995, **95**, 1431.
38 E. Lindner, R. Schreiber, T. Schneller, P. Wegner, H. A. Mayer, W. Göpel and C. Ziegler, *Inorg. Chem.*, 1996, **35**, 514.
39 I. B. Berlman, *J. Chem. Phys.*, 1970, **52**, 5616.
40 B. Lehr, H.-J. Egelhaaf, H. Fritz, W. Rapp, E. Bayer and D. Oelkrug, *Macromolecules*, 1996, **29**, 7931.
41 B. Lehr, H.-J. Egelhaaf, W. Rapp, E. Bayer and D. Oelkrug, *J. Fluorescence*, 1998, **8**, 171.
42 J. Michl and E. W. Thulstrup, *Spectroscopy with Polarised Light*, Wiley-VCH, Weinheim, Germany, 1995.
43 G. G. Aloisi, F. Masetti and U. Mazzucato, *Chem. Phys. Lett.*, 1974, **29**, 502.
44 G. G. Belford, R. L. Belford and G. Weber, *Proc. Natl. Acad. Sci. USA*, 1972, **69**, 1392.
45 R. K. Harris and R. H. Newman, *Mol. Phys.*, 1979, **38**, 1315.
46 D. R. Bauer, J. I. Brauman and R. J. Pecora, *J. Am. Chem. Soc.*, 1974, **96**, 6840.
47 *CRC Handbook of Chemistry and Physics 1999–2000*, 80th edn., ed. D. R. Lide, CRC Press LLC, Boca Raton, 1999.
48 A. Szabo, *J. Chem. Phys.*, 1984, **81**, 150.
49 P. Wahl, *Chem. Phys.*, 1975, **7**, 210.
50 W. A. Wegener, R. M. Dowben and V. J. Koester, *J. Chem. Phys.*, 1980, **73**, 4086.
51 G. Cerveau and R. J. P. Corriu, *Coord. Chem. Rev.*, 1998, **180**, 1051.
52 A. Katz and M. E. Davis, *Nature*, 2000, **403**, 286.